Angles-Only Orbit Determination Accuracies with Limited Observational Arc

Kyle Stoker, James Johnson, Kira Abercromby
California Polytechnic State University, San Luis Obispo

Liam Smith, Morgan Yost, Andrew Zizzi
Lockheed Martin Space Systems Company

CONFERENCE PAPER

Space situational awareness (SSA) has become a more complex problem to understand with the recent influx of trackable orbital debris and passive small satellites into Earth-orbit. Maintaining an accurate catalog of all objects in orbit is imperative for understanding the space environment and allowing for precautionary measures to be taken well in advance of any threat of collision between objects. As the sensitivity of ground-based observation facilities increases to be capable of tracking and cataloguing smaller objects in orbit, the limitations of orbit determination methods must be well understood to account for the errors present in initial estimates of an object's orbital state. This paper analyzes the effectiveness of angles-only orbit determination methods when limited observational data is available on an object, with the hope to predict the magnitude of the state error given the amount of observational arc. The analysis uses data obtained from Lockheed Martin's Space Object Tracking (SPOT) facility; whose optical instrumentation is capable of both slewing fast enough to track objects in LEO while also having the sensitivity to detect faint objects in GEO. It was found that below 5 degrees there is greater difficulty in reliably predicting a secondary pass of an object, and that the error in each IOD method shows a strong correlation with the amount of observational arc seen.

1. Introduction

The increasing number of objects in Earth-orbit over the last decade has placed an emphasis on having up-to-date coverage and tracking of debris in space, as the risk of collision between objects can be minimized through knowledge of the constantly evolving debris environment. While there are many objects that orbit the Earth, the most populated orbital regime is the Low Earth Orbit (LEO) regime at 71.9% of all currently tracked objects. Furthermore, satellites are being launched at an increased rate. Commercial companies like SpaceX, OneWeb and Amazon have announced development on "Mega Constellations" that consist of thousands of LEO satellites, with SpaceX's Starlink project already approved for 12,000 satellites by the FCC. This increased demand for object tracking from ground stations will require additional tracking infrastructure or shorter observation periods. With a limited number of facilities dedicated to tracking Earth bound objects, the amount of observation time for each object is often sacrificed in order to observe more objects at shorter intervals. Because of this, it is important to understand how the different IOD methods behave in the LEO regime with short observational arcs to help assist in the observation and tracking of uncatalogued debris. This paper analyzes the effectiveness of angles-only orbit determination methods when limited observational data is available on an object, with the hope to predict the magnitude of the state error given the amount of observational arc.

This study was performed using observational data from Lockheed Martin Space's Space Object Tracking (SpOT) facility[4]. The facility consists of three raven class 1-meter telescopes, with the goal of tracking and characterizing current space assets and debris. The SpOT facility is both an operational Space Situational Awareness (SSA) facility and a test bed for advanced sensor research and development. The telescopes at the SpOT facility are capable of slewing fast enough

to rate track LEO satellites, while also having enough optical power and sensitivity to detect dim objects in GEO. Lockheed Martin has collected high frequency observational data and has allowed Cal Poly use of selected objects of interest for this project.

2. Orbital Pass Geometry

It is important to understand the geometry of orbital passes and the requirements for an object to be observed from an optical ground station. In order for an object to be observed by an optical system, the object being observed must be illuminated by the sun and meet brightness requirements for the telescope, the observation site must be dark enough to see faint objects, and the object must be above the horizon of the observation site[J14]. These factors play heavily into the limited ability to collect observational data for LEO objects.

For an object to be illuminated by the sun, the only requirement is that the object is not in the Earth's shadow. If the perpendicular distance from the centerline of the Sun to the object is greater than the Radius of Earth, then the object is illuminated by sunlight, with the possibility of being observed. The next condition to evaluate is whether the observing site is being illuminated by sunlight. If the dot product of the Sun vector and the observation vector, both in ECI, is negative, then the site is not illuminated by the sun. Practically, this requires the sun to be further below the horizon for it to be dark enough to observe. Gasdia[3] notes that a good rule of thumb is starting at nautical twilight, when the sun's center is 6 degrees below the horizon. After reaching this angle, it is dark enough to observe objects until the maximum angle below the horizon for the orbit is reached, which can be calculated using the Equation:

$$\Delta = cos^{-1}\left(\frac{R_\oplus}{R_\oplus + h}\right)$$

For LEO objects, defined as having altitudes of 100 to 2000 km[3], the maximum angle below the horizon is 10 to 40 degrees. Since Earth's angular velocity is roughly 15 degrees/hour, this corresponds to one to three hours of observing time for LEO objects. The final requirement is that the object is above the horizon of the observing site. To determine whether the object is above the horizon, the z-component of the slant range vector in the Topocentric Horizon frame must be positive. These three conditions drastically limit the amount of opportunities for observations for optical systems. Other systems, like radar, don't care whether the object is illuminated by the sun or if the observation site is in darkness. For LEO objects with periods ranging from 85 to 130 minutes, this limits

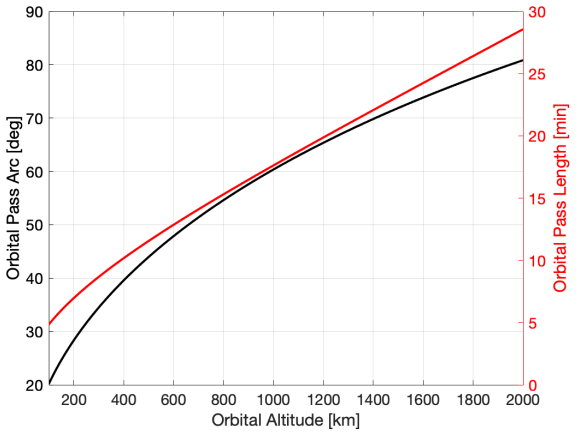

Fig. 1: Length of Orbital Pass Based on Altitude

observations to 1 to 2 passes per morning and evening observation session. This assumes that the object is overhead during those times, so in reality, the number of observing passes is much less.

The other aspect to consider besides the frequency of orbital passes is the quality of orbital passes. For any orbital pass, the pass that maximizes the amount of time the object is visible will pass directly overhead of the observer[3]. This corresponds to the observer being directly on the ground track of the object. Figure 1 shows the amount of orbital arc and the amount of time an observer would see during a maximum duration pass for different orbit altitudes. For passes that are not directly overhead, the amount of orbital arc that is seen and the amount of time will be less. Other considerations are that at low elevation angles, optical systems are seeing through more of the atmosphere, causing measurement error to be higher. At lower elevation angles, the range between the object and the optical system is the highest, which causes the brightness of the object to be lower due to the fact that

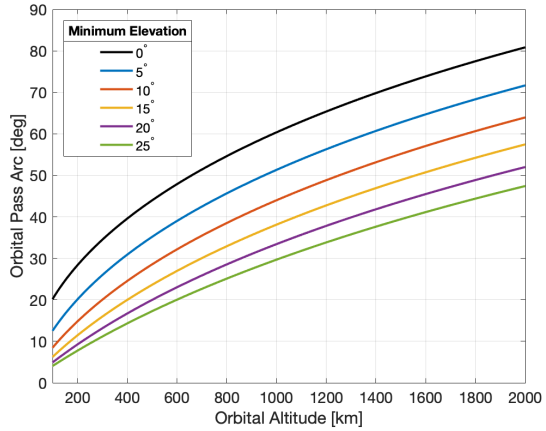

Fig. 2: Change in Orbital Arc with Elevation Mask

the intensity of the object-reflected light varies by 1/d2[J14]. Another consideration is that objects on the horizon, such as mountains or man-made structures, can interfere with the minimum elevation angle. Finally, there is some time required for optical systems to acquire the object and take early measurements. All of these factors can manifest themselves into an elevation mask for an observation site; by limiting the minimum elevation angle to start an orbital pass, the amount of orbital arc and observing time will decrease. Figure 2 shows the effect of adding different minimum elevation angles on the amount of orbital arc seen on a maximum duration pass. These real-world limitations of non-ideal orbital passes combined with the limited number of observable passes due to visibility requirements drastically limit the amount of data that can be collected for LEO objects.

3. Methodology and Analysis

The first approach to better understanding IOD accuracies for LEO debris that was undertaken for this paper involved focusing on rocket body debris data that was provided by SpOT, with data from 15 different rocket bodies that had been observed by SpOT being made available for use in this paper. The focus for these data sets was to identify the accuracy that can be achieved with IOD when limited to a short orbital arc of data. Once this accuracy is better understood through data testing, it is then important to know if the level of accuracy achieved by the IOD methods would allow for follow-up observations to be made of the objects. Follow-up observations for LEO objects are inherently difficult due to the limitations of optical space observation that were mentioned above but being able to achieve a second set of observations for an object can aid in an object's orbit being more accurately defined, and eventually catalogued as a known object in space. While the focus of this analysis is catalogued rocket body debris, the same process can be applied to debris objects of unknown orbit and origin such that they can likewise be catalogued in the future.

The rocket body debris objects made available by Lockheed Martin for use in this paper had dozens of passes worth of data in which to analyze; however, the observational time period for one pass of a rocket body object ranged anywhere from a few seconds up to one minute in length. During preliminary data testing, IOD results using observational data that lasted only a few seconds were highly inconsistent and inaccurate compared to the longer observation times. This led to the decision to only perform analysis on object's where the observation time exceeds 50 seconds.

A lower threshold would give more inaccurate results than desired and does not give a realistic representation of the observational capabilities of the SpOT facility. A higher threshold would limit the analysis to only a few objects, as the maximum observational period from the available data was approximately 60 seconds long. The 50 second threshold balanced the two factors of wanting accurate results while still having a large enough sample size for worthwhile analysis. All in all, there were 50 instances of object passes with observation times in the 50 to 60 second range, and these 50 observational passes constitute the data for the first section of analysis and results within this paper. As mentioned previously, the original data available was of 15 rocket bodies, but only nine of these rocket bodies had observational passes that met this 50 to 60 second criteria. Thus, nine rocket bodies and 50 total passes will encompass the final analysis of the paper with regard to the rocket body debris objects.

In order to understand the inherent error present in an initial orbit determination solution, a true orbital solution must be known and used as comparison. The baseline solution will be historical TLE data for the observed rocket bodies, whose orbital ephemeris can be propagated to the observation times and directly compared in terms of its orbital state and elements. While there will be no comparative benchmark in which to qualify results when attempting to analyze untracked debris, it is a necessary comparative tool in order to better understand the accuracy one can expect from an initial orbit determination solution. Once this expected accuracy is better understood, this knowledge can be applied to situations where there is no TLE data to reference and can help assist in the observation and tracking of uncatalogued debris.

The scheme for IOD that will be applied to the rocket body SpOT data and analyzed for its accuracy is an assumed-circular orbit (ACO) Gaussian IOD. As seen in its name, this method will assume that the object being observed is in a circular orbit, and the Gaussian IOD estimate will be forced into an orbit that is approximately circular. On the surface, this appears to only be beneficial if the object being observed is known to be in a near circular orbit. However, an object does not need to have a zero eccentricity for an ACO solution to give a good estimate of an object's orbit, as will be seen later.

The fundamental change that is needed in order to transition from a traditional Gauss IOD towards an ACO Gauss IOD lies within the velocity vector solution that results from the Gauss method itself. The traditional Gaussian velocity vector solution has no bounds on it, and the magnitude and direction of this vector along with its accompanying position vector can give a solution that has any range of eccentricities.

To force the solution into a circular outcome, the first step is to look at the position vector output of the

Gaussian IOD solution. If the object was in a circular orbit, the velocity magnitude can be calculated using the equation:

$$|v_c| = \sqrt{\frac{\mu}{|\vec{r}|}}$$

This equation gives the magnitude of velocity of the object if assumed to be in a circular object. In order to obtain a velocity vector, not just a magnitude, it is required that a unit vector is obtained for the direction that the velocity vector is pointing in. With the magnitude and unit vector, the velocity vector can be obtained through the following relationship:

$$\vec{v}_c = |v_c|\hat{v}$$

Fortunately, the unit vector can be obtained directly from the velocity vector of the original Gauss solution before any circular assumptions were made. The velocity vector result that stems from the IOD solution will have a certain magnitude and unit vector that correlates to the orbital solution arrived upon. This unit vector is representative of the direction that the object's velocity is pointed and can be used to obtain the desired velocity vector of the object under an assumed-circular orbit restriction. Combined with the original position vector solution of the Gauss IOD algorithm, this new velocity vector results in an orbital solution for the observed object that is approximately circular.

Utilizing an assumed-circular orbit approach to the initial orbit determination of the data is not the only way to potentially increase the accuracy of the IOD solutions. The SpOT telescope system is capable of tracking and recording data for observations at an extremely fast rate, resulting in hundreds and sometimes thousands of data points for one object during an overhead pass. Finding a way to utilize more than just three data points, which is all that is required for a single IOD solution, could potentially increase the accuracy of the IOD results when comparing them to TLE data.

After preliminary testing with a simple Gaussian three-point IOD method, one initial takeaway was that the IOD orbital solution when using three points over such a short time span gave extremely inconsistent results. One IOD solution using three points at t = 0, 25, and 50 seconds may give a poor result as compared to the TLE solution, whereas using the subsequent data points at t = 0.025, 25.025, and 50.025 gave a much more accurate result, despite no apparent difference in the quality of these data points. An iterative approach to the data was created in order to refine the accuracy of the IOD results by using as many data points as possible, aiming to reduce the inconsistency seen from one three-point IOD solution to the next.

The basis of this method involves grouping the beginning, middle, and end sections of one data set into three separate groups. The first group of data at the beginning will only be used as the first point in a three-point IOD solution, the second grouping in the middle will only be used as the second point of the IOD solution, and the third grouping will only be used as the third point of the IOD solution. By performing a three-point IOD solution for every combination of data points in groups 1, 2 and 3 and averaging these solutions at a shared epoch, a more accurate result could potentially be achieved.

To better understand this, it is best to look at a specific example of how this was implemented. The data set for one pass of an SL-3 rocket body debris (NORAD ID 00877) lasted 59.1 seconds and contained 1183 observation points with a separation of 0.05 seconds between each data point. This data was then grouped into three groups: group 1 contained the first 50 data points from t = 0 to t = 2.5 seconds, group 2 contained the 50 data points from t = 25 to t = 27.5 seconds, and group 3 contained the 50 data points from t = 50 to t = 52.5 seconds. For simplicity, let the data in group 1 be represented by the values 1.1, 1.2, up to 1.50, the data in group 2 be represented by 2.1 up to 2.50, and the data in group 3 be represented by 3.1 up to 3.50.

With the data separated, the process of iterating through each combination of these data groups can begin. Starting with the grouping [1.1, 2.1, 3.1], Gaussian IOD was used to calculate a three-point IOD solution for the object, with the assumed-circular orbit approach that was described earlier. The next grouping would be the data points [1.1, 2.1, 3.2], and a separate result using Gaussian ACO IOD is calculated. This process iterates through all possible combinations of the three groupings of data, which in this example would be 50x50x50 iterations, or 125,000 iterations and 125,000 unique IOD solutions from one observational set of data. At this point, all of these solutions can be propagated back to a single time at t = 0 seconds (which is the first point of the data set after the processing that was described in Section 3.4), and their position and velocity magnitudes averaged to create one nominal IOD estimate for the object. Because of the short timespan needed for propagating each solution (around 25 seconds), a two-body propagative model is used to propagate each solution to the initial observation time, as perturbational effects should be negligible.

Because both the number of data points and the gap between data points was not uniform for all of the data provided by the SpOT facility, a consistent method of grouping each set of data was difficult to achieve. The goal was to group data into three sets of 50 observation points for the iterative method,

however, sometimes less points needed to be chosen in order to maintain an approximate 50 second gap for each IOD iteration. No single iteration calculated an IOD solution using less than 45 seconds of orbital arc, nor greater than 55 seconds of orbital arc, so as to keep the results of each individual IOD solution in that will be averaged to a nominal solution comparable to one another. Additionally, with some data sets only lasting around 51 or 52 seconds in length, the number of data points available for the third grouping was limited, and less iterations could be achieved. An overview of the groupings and iterations chosen for all 50 data sets is shown below in Table 1. With some limitations in certain data sets, nearly 80% of the data could still be iterated on 125,000 times while maintaining the requirements mentioned above.

Table 1: Grouping of Data for Iterative ACO Scheme

Data Grouping	Occurrences	Iterations
11 x 11 x 11	2	1,331
25 x 25 x 25	1	15,625
30 x 30 x 30	2	27,000
40 x 40 x 40	6	64,000
50 x 50 x 50	39	125,000

After understanding how the IOD methods performed at a fixed observation interval, the amount of orbital arc that was seen by each IOD method was changed. This would show if the amount of orbital arc had an effect on the accuracy of the IOD solution. Each orbital pass was often hundreds to thousands of data points depending on the orbital pass, and since the angles only IOD methods being studied only use three data points, specific data points must be picked systematically. To make sure that each IOD solution is comparable to another, the second observation should be the same for every grouping of three observations. This allows for the IOD solutions to be compared directly, greatly simplifying the analysis process. The second observation was chosen to be the measurement made halfway through the pass. A percentage of the orbital pass determined the first and third measurement, ranging from 100% being the entire pass and as low as 5-10% for a very short period of the orbital pass. By varying the first and third observation while keeping the second observation fixed, the amount of orbital arc seen by the IOD method can be controlled and the IOD results can be directly compared without the need for propagation.

The following method for quantifying orbital error was first proposed by Mortari[5] and utilized extensively in Schaeperkoetter[6]. The error method reduces the number of parameters from 6 to 2, with the option to combine into a complex number to have a single parameter.

The first parameter is the shape error. This value determines how well the estimated orbit's shape matches the true orbit, regardless of the orbital plane. The calculation uses the semi-major axis and eccentricity to calculate the semi-minor axis:

$$b = a\sqrt{1 - e^2}$$

Both a and b are distance values that are dimensionally consistent. Thus, the distance between the true orbit parameters, a_o and b_o, can be taken to determine the orbital shape error:

$$E_{shape} = \sqrt{(a - a_o)^2 + (b - b_o)^2}$$

The second parameter is orientation error. This value is the principle rotation angle between the estimated orbit frame and the true orbit frame. The rotation is defined by inclination, right ascension of ascending node, argument of perigee and true anomaly to describe the transformation from the inertial reference frame to the rotating orbital reference frame. This transition matrix is defined as:

$$C = Rot_3(\omega + \nu)Rot_1(i)Rot_3(\Omega)$$

Once the transition matrix is developed for both the estimated orbit and the true orbit, C and Co respectively, the orientation error can be calculated by finding the principle rotation angle between the two transition matrices, seen in Equation (J3.10):

$$E_{angle} = cos^{-1}\left(\frac{1}{2}\left(trace\left[CC_o{}^T\right] - 1\right)\right)$$

This simplification of six parameters down to two parameters greatly reduces the amount of information required to analyze, while still giving helpful information compared to the Cartesian system.

The period of an orbit is the amount of time it takes to make one complete revolution and is directly related to the semi-major axis of the orbit. Period error manifests itself as an object leading or lagging behind the true position. A positive period error correlates to a larger semi-major axis, and the object will be behind its expected position. Similarly, a negative period error correlates to a smaller semi-major axis, and the object will be in front of its expected position.

Angles only IOD methods are not accurate enough for long term predictions, so in order for more accurate orbit estimations to be generated, another orbital pass must be observed to increase the accuracy. However, if the angles only IOD methods are not able to produce

an accurate enough solution to predict future observations, then the estimation is not useful. Because of this, it is important to propagate forward the orbit estimations from IOD methods to the next observable pass to determine if they are accurate enough to facilitate more observations. Observational angles will be generated from the propagated state to determine if the orbital estimate was accurate enough to be within the field of view of the optical system.

To calculate observation angles from the state first requires determining the slant range vector:

$$\vec{\rho} = \vec{r} - \vec{R}$$

Once the slant range vector is found, it is converted to a pair of observation angles. Coming from slant range, Declination is defined as:

$$\delta = sin^{-1}\left(\frac{\rho_z}{|\rho|}\right)$$

and Right Ascension is defined as:

$$\alpha = cos^{-1}\left(\frac{\rho_x}{|\rho|\cos(\delta)}\right) \qquad when\ \rho_y > 0$$

$$\alpha = 360° - cos^{-1}\left(\frac{\rho_x}{|\rho|\cos(\delta)}\right) \qquad when\ \rho_y < 0$$

For these observation angles, if the right ascension and declination error are both less than half of the field of view, then the orbit estimate is accurate enough to facilitate more observations and is considered a successful case. However, if the orbit estimate has period error, this will result in the object leading or lagging behind its expected position. If the IOD method was able to define the orbital plane well, but is simply off on the shape, i.e. semi-major axis and eccentricity, then observing it slightly before or slightly after the expected time is still possible. To account for this fact, if at any point on the interval ($t_o - E_{period} \leq t_o \leq t_o + E_{period}$) that the condition is satisfied, this will also result in a successful case. This translates to pointing the optical system at the expected observation point and waiting until the object passes into view. This can be seen in Figure 3.

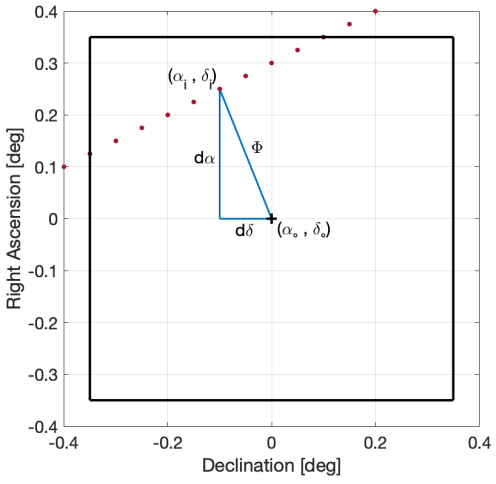

Fig. 3: Field of View Limits to Observe and Object

4. Results

When working with very short arc observational data in the pursuit of initial orbit determination results, IOD solutions that are not reasonable are often times unavoidable. While Gaussian IOD is a strong method of choice for short-arc observational data, it can still provide IOD solutions that are unreasonable or unrealistic. When performing the iterative ACO initial orbit determination method on the 50 rocket body data sets for this paper, three of the data tests tested could not solve to a solution, and two more resulted in Not a Number (NaN) solutions due to a singularity issue that can arise as part of the Gauss IOD algorithm. The limitation of using extremely short arc observational data for IOD is something to be fully aware of for future applications. With five total data sets providing unusable results, the analysis and results that follow will focus on the results of the 45 data sets that provided reasonable and realistic IOD solutions.

The median and mean errors of all 45 data sets can be seen below in Table 2 and Table 3, highlighting that the orbital plane elements of inclination, right ascension of ascending node, and argument of latitude are accurately solved for using the Gaussian ACO initial orbit determination method. Additionally, the median position error is below 40 kilometers, which is a good estimate for an object given only approximately 50 seconds of orbital arc.

Table 2: ACO IOD State Error

	Mean Error	Median Error	Mean % Error	Median % Error
$\mathbf{R_x}$	26.7 km	18.3 km	2.18	0.55
$\mathbf{R_y}$	29.9 km	22.8 km	0.88	0.60
$\mathbf{R_z}$	23.9 km	12.5 km	0.56	0.31
$\mathbf{\lvert R\rvert}$	54.3 km	39.4 km	0.76	0.55
$\mathbf{V_x}$	50 m/s	35 m/s	1.89	1.21
$\mathbf{V_y}$	55 m/s	37 m/s	2.48	1.32
$\mathbf{V_z}$	41 m/s	20 m/s	1.31	0.54
$\mathbf{\lvert V\rvert}$	98 m/s	63 m/s	1.30	0.84

Table 3: ACO IOD Orbital Elements Error

	Mean Error	Median Error	Mean % Error	Median % Error
h	525.7 km^2/s	270.5 km^2/s	0.98	0.50
i	0.182°	0.146°	0.31	0.24
Ω	0.325°	0.331°	0.13	0.10
u	0.171°	0.115°	0.29	0.26
e	0.008	0.004	117.8	35.22
a	142.8 km	73.3 km	1.97	1.02
T	3.01 min	1.54 min	2.96	1.53

The main goal of many initial orbit determination applications for debris objects is to provide a level of accuracy needed to allow for the object to be observed again on subsequent flyovers overhead. One of the main contributors to an object feasibly being observable during subsequent orbits is the orbital period error of the IOD solution, as the predicted timing and observation pointing direction of a telescope are directly related to the period of the object being observed. To understand if the results of the 45 test cases that were analyzed would provide results accurate enough to allow for follow-up observations of an object to take place, a specific test case from the data sets can be analyzed to better understand the feasibility of reacquiring the target object in the future.

The analysis will focus on the 22nd data set that successfully was tested from the rocket body dataset, which will be referred to as Test Case 22. Test Case 22 is one of the observational passes of rocket body debris object NORAD 02802, which at the time of observation had a very low eccentricity of 0.0058. Analyzing this test case and its IOD results will give insight into the feasibility of cataloguing debris in near-circular orbits using the developed iterative ACO IOD method. Table 3 shows the IOD errors for Test Case 22 compared to the TLE data for R/B 02802 at the time of observation.

Table 3: Test Case 22 ACO IOD Error

	ACO IOD Error
|R|	26.5 km
|V|	63 m/s
i	0.201°
Ω	0.244°
u	0.124°
T	0.638 min

The relative errors of the IOD solution are low for all of the variables in Table 5.1, most notably only having an orbital period error of 38 seconds compared to the TLE orbital solution for the rocket body debris object. While calculating and analyzing the error values for the IOD results is a good way to see the accuracy of the IOD method, these raw values do not give any meaningful insight into whether the error in the IOD solution is small enough as to allow for follow-up observations. To get insight into this, both the TLE orbital state and ACO IOD solution state were propagated forward in time using the SGP4 orbital model in AGI's Systems Tool Kit, and then analyzed for the growth in error over time between the two propagated orbits. Figure 4 below shows the right ascension and declination angles of both the TLE and ACO IOD solutions over a two-hour period after the time of first observation of R/B 02802 for Test Case 22, focusing on when the rocket body object was visible overhead.

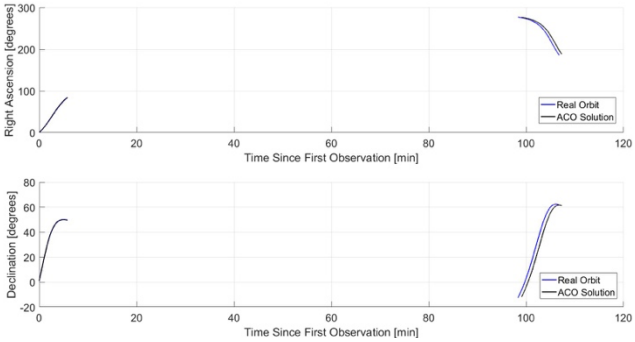

Fig. 4: Test Case 22 Right Ascension and Declination Comparison

Both the right ascension and declination of the two propagated orbits match up well with each other during the first overhead pass when the object is first observed, which is shown in the first 5-minute span of Figure 4. When the object becomes visible overhead of the observation location once again near the 100-minute mark, the angles are more noticeably separated, but are still very close to each in overall trend but shifted in time. This shift is caused by the orbital period error between the ACO IOD solution and the true orbit of the object as depicted by the TLE propagated solution, as the IOD solution has a slightly longer orbital period, and thus becomes visible overhead slightly later than the actual orbit of the rocket debris object.

To understand the feasibility of finding the actual object using the ACO IOD solution, it must be determined if the object will pass through the telescope's field of view if the telescope is pointed at the right ascension and declination of the IOD solution

when it becomes visible on its second pass overhead. For the object to pass through the telescope's field of view, which is 0.7-degrees for the telescopes at the SpOT observational facility, the error between both the right ascension and declination angles must thus be below 0.35-degrees simultaneously at any point during the object's overhead pass. To see if this occurs at any point during the propagated orbits of the ACO IOD solution and the TLE solution, a right ascension and declination telescope pointing angle was chosen at t = 100 minutes, as the ACO orbit has definitively become visible overhead at this point in time. With these two values chosen, the error between this telescope pointing direction and the observational angle values of the true orbit, as depicted by the TLE solution, can be calculated for the entire duration of visibility for the second overhead pass.

Figure 5 shows the error in both right ascension and declination between the object passing overhead and the chosen telescope pointing direction.

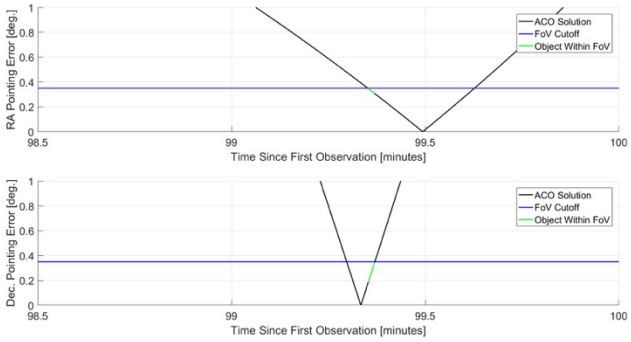

Fig. 5: Test Case 22 Theoretical Telescope Pointing Error

The blue horizontal line represents the field of view cutoff point for the SpOT telescope system, and as shown by the highlighted green portion on both the right ascension and declination plots, there is a period of time where both of these two angles fall below the necessary pointing error requirement such that the rocket body debris object would pass through the telescope's field of view. This period of time is brief, only lasting 1 second, but can be the basis of the telescope system reacquiring and tracking the rocket body debris object overhead. The main limiting factor of this short period of visibility in the telescope's field of view is the telescope's FOV value itself. When rerunning this scenario using a slightly increased FOV value for the telescope, 1.0 degrees, the time period of visibility for the object increases to 5.6 seconds. Having a higher FOV telescope can bring the added benefit of increasing the likelihood of finding an object as well as extending the period of visibility for that object, but must be weighed against the drawback of losing telescope sensitivity for wider-FOV optical telescope systems.

The analysis for this specific test case shows that there is definite potential and feasibility in using a short-arc optical observation data set for a debris object to perform accurate initial orbit determination in the pursuit of obtaining follow-up observational data for the same debris object, wherein the IOD results can be further refined and their accuracy improved through other precise orbit determination methods, which is outside the scope of this paper.

There are caveats to this analysis that should be understood before performing future work on the subject matter. First, this analysis assumes that follow-up observations can be made on consecutive passes of a debris object. The two limiting factors for this being achievable are observational windows for optical telescopes, and ground track geometry. To maximize the potential for getting two observational data sets of one object during the same observational window, the first observation of a debris object must occur as early in the observation window as possible. With LEO objects having orbital periods averaging 90-100 minutes, and an observational window for LEO optical observation lasting two to three hours at most, the first observation must occur early on so that the second overhead pass will occur during the same observation window. Regarding ground track geometry, prograde LEO orbits drift to the West from one orbital ground track to the next, meaning the first observation of a debris object must occur East of the observation location, so that the subsequent orbit of the object will still be visible from the ground station during its next pass.

Additionally, it is important to understand that the object in Test Case 22 would pass through the telescope's field of view but would not do so at the predicted time due to the orbital period error within the ACO IOD solution. While this difference is less than one minute, it is important to recognize that an IOD solution with such a small orbital arc of data will not be perfect, and the observation system will need to be flexible and robust enough to identify the object even if it does not pass through the telescope's field of view at the exact predicted time.

Even with these limitations that must be considered, utilizing optical initial orbit determination shows great promise for being able to not only obtain accurate initial orbital solutions for debris, but can also provide a user with a level of accuracy required to obtain future observational data for a debris object, at which point other orbit determination methods can be applied to refine the orbit of the object.

Next, the results focus on the variation in error metrics when the amount of orbital arc is varied. The following graphs come from Test Case 10. For the orbital plane definition, which is based on inclination, right ascension of ascending node, argument of perigee and true anomaly, all of the angles only IOD methods are able to define the orbital plane to around the same level of accuracy. There was no one method that had the greatest accuracy in defining the orbital plane. The amount of error in the orbital plane showed to be very consistent as the amount of orbital arc changed. The Orientation error, seen in Figure 6, show that the angles only IOD methods are fairly consistent

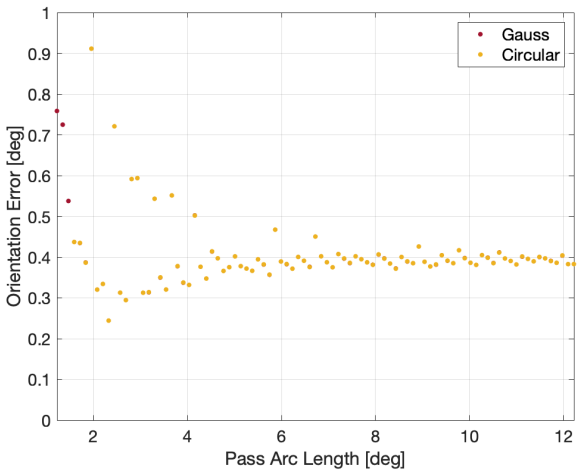

Fig. 6: Test Case 10 Orientation Error

in their estimation of the plane orientation for the orbit, regardless of the amount of orbital arc that was seen. Since the Circular method uses the position vector of the Gauss method, the Circular method is defined by having the same orbital plane as the Gauss method, so the orientation error for the Circular method also matches the Gauss method.

When looking at the shape error, the Circular method provided the greatest results. The Gauss method failed to give a reasonable estimate below 5 degrees, whereas the Circular method is very consistent as the amount of orbital arc changes. For Test Case 10 specifically, it was more accurate at the smaller amounts of orbital arc. Shape error, which is dependent on the semi-major axis and eccentricity is greatly affected by the magnitude of the velocity vector, so when the velocity error is high, the shape error also degrades.

When taking both shape and orientation error into account in the short arc regime, the Circular method provided the greatest results. The orientation error showed to be very consistent as the amount of orbital arc decreased. When the methods converged, the average orientation error was between 0.7 to 0.9

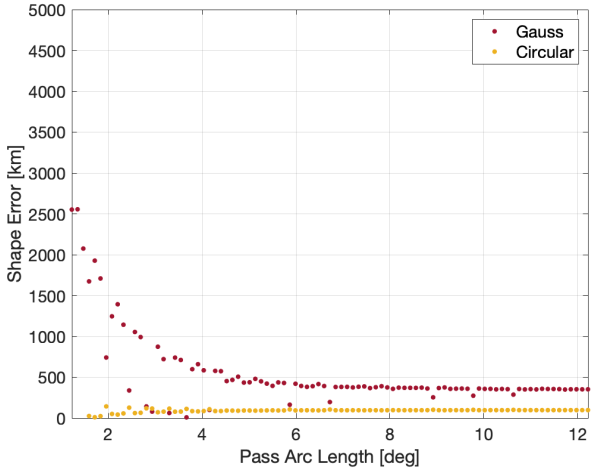

Fig. 7 Test Case 10: Shape Error

degrees, with each method having some Test Cases in which they performed the best. No method provided a solution that had the best orientation error consistently from pass to pass.

Like the shape error of an orbit, the orbital period is directly dependent on the semi-major axis of the estimated orbit. Thus, incorrectly estimating the semi-major axis will result in a period error, which causes the object to lead or lag behind the expected position. This has the largest effect in predicting the next orbital pass of the object to observe it for a second time. The orbital period error, seen in Figure 8, tends to diverge from the true period as the orbital arc seen decreases. The Circular method is consistent in giving a good period estimate that is close to the true orbit, whereas the Gauss method is consistently off in its prediction of the period, which stems from the method's difficulty in estimating the velocity vector.

When trying to predict the observation angles for the next orbital pass, which will be discussed more in

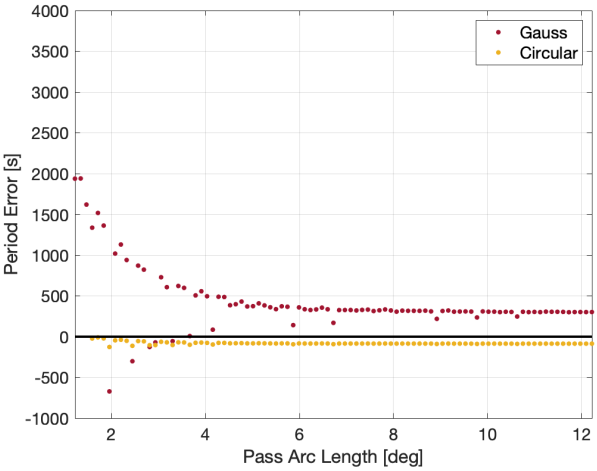

Fig. 8: Test Case 10 Period Error

the following section, low period error is necessary to observe the object for a second time. Since LEO objects are constrained to 2-3 orbital passes per observing session due to the orbital pass geometry of seeing and observing an object, missing the secondary pass will result in an ineffective IOD solution for long term prediction. After the first observation session, it is often impossible to predict the object's location from the original IOD solution if it has not been improved with a secondary pass. This is mainly due to the fact that period error is additive for each orbital pass. A period error of 100 seconds, which is not uncommon considering the period error seen in Figures 4.10 and 4.11, over the span of 10 orbital revolutions would leave the object 1000 seconds behind its true position. Since there is no way to determine if the period error is positive or negative without knowing the true orbit, the object could lead or lag by as much as 1000 seconds. This would drastically decrease the efficiency of any observing site if telescopes had to observe for that large of an interval before and after an orbital pass in order to observe an object again.

The accuracy of the observation angles on a secondary pass are shown in Figure 9.

If both the right ascension and declination error are smaller than half of the field of view of the optical system, an observation can be made. For Lockheed Martin's SpOT Facility, the optical systems have a 1 meter primary mirror that has a 0.25 degree field of view, and a 106 millimeter spotter scope that has a 0.7

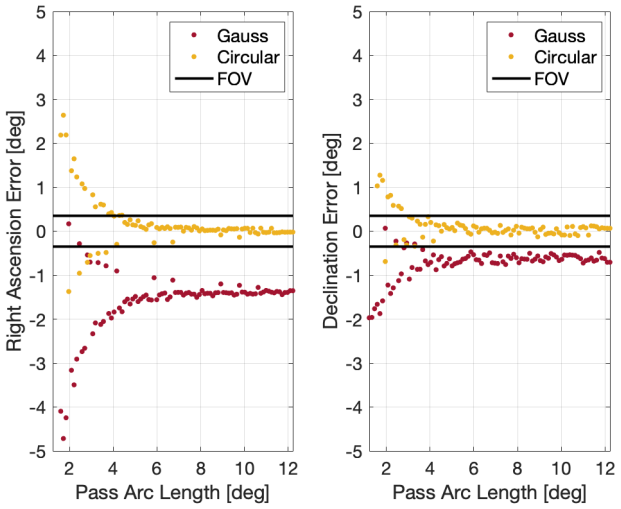

Fig. 9: Test Case 10 Right Ascension and Declination Error

degree field of view that is used during acquisition[47]. Thus, right ascension and declination error must both be below 0.35 degrees for an initial observation to be made for the SpOT Facility. Table 4.8 shows the number of successful predictions that each method produced over the 15 orbital passes analyzed. There were 7 orbital passes that had a maximum orbital arc that was greater than 5 degrees, so they were analyzed in both cases, which is why all 15 cases where checked in the $\theta < 5^\circ$ regime, whereas only 7 cases where checked in the $\theta > 5^\circ$ regime. Some methods, such as Gooding, Gauss and Double-R, are within the tolerance for some orbits and not within tolerance for other orbits. Only the Circular method was able to predict secondary passes reliably. This should not be surprising because of the way the Circular method is designed. Since the velocity vector is constrained by the definition of a circular orbit, the error in the Circular method is dependent on the positional error only, not both the position and velocity error. Since the error in the position is proportionally smaller than the velocity error, the Circular method does perform better on average compared to the other methods. However, on passes that were less than 60 seconds, which corresponds to around 4 degrees of orbital arc, none of the methods were able to produce reliable IOD solutions that could predict a secondary pass. Once again, this shows the importance of collecting as large of an orbital pass as possible in order to have the greatest chance for a secondary observation.

5. Conclusion

Utilizing the rocket body debris data from the Space Object Tracking Facility, consisting of nine different target objects and 50 passes of data total (with 5 of these 50 passes discarded due to poor or no results), relative initial orbit determination accuracy values were determined for an iterative assumed-circular orbit method. The iterative ACO method performed well across all 45 successful data sets, with low error values for position, velocity, orbital plane, and orbital period. With the IOD accuracies better understood for the rocket body debris data, a feasibility analysis was conducted looking into the potential of one optical observation facility being used to observe and catalog untracked debris. The results of this analysis were promising, as a test case was shown to produce an IOD result that was accurate enough to allow for a follow-up observation to be made, under the correct circumstances. To build upon the promising results that were found, future work on this subject could include applying the iterative ACO method and observation procedure to a real scenario, attempting to observe an object during a pass overhead, followed by performing IOD on the resultant data, and lastly using the IOD results to acquire the target object overhead on its next overhead

pass. If this process is shown successful, such a system could be applied to the task of identifying and cataloguing untracked debris objects.

The IOD methods performed remarkably well considering the limited amount of data to process. While the Gauss method and the Circular method both produced solutions with orbital arc below 5 degrees, the Assumed Circular method provided the most consistent results in the ability to estimate the orbit with limited data. All of the methods were able to determine the orbital plane consistently within 1 degree of the true orbital plane, regardless of the amount of orbital arc seen. This means that the ability to predict a secondary orbital pass is determined more on the shape of the orbit, and the most effective IOD methods are the ones which define the orbital shape the best. As the amount of orbital arc decreased, the shape error and period error increased at an exponential rate. The velocity error adversely affects the semi-major axis and eccentricity of the resulting orbit solution, which causes large discrepancies between the estimated period and the true period. If this period error is not accounted for, the success of a secondary observation session is very low; however, when taking the period error into account to develop a time interval for initial acquisition, the Circular method is very consistent in predicting the secondary observation session. This was only the case when the orbital arc observed was greater than 5 degrees, otherwise all of the methods could not consistently predict a secondary pass. If the FOV requirements of the system are relaxed, such as using multiple telescopes to create an optical fence to increase the FOV or slewing the telescope at different rates to increase the observation probability, then the amount of successful observations would increase. The strict FOV requirements were put in place to allow for more flexibility for observers who have other techniques to increase the observation chances on a secondary pass, as well as to analyze the "worst case" error metrics. Thus, for angles only IOD to produce effective solutions conducive to predicting secondary passes, collecting as much of the orbital pass as possible needs to be a priority.

References

[1] K. Stoker. Initial Orbit Determination Error Analysis of Low-Earth Orbit Rocket Body Debris and Feasibility Student for Debris Catalonging from one Optical Facility. California Polytechnic State University, San Luis Obispo, 2020.

[2] J. Johnson. Limitations of Initial Orbit Determination Methods for LEO CubeSats with Short Arc Orbital Passes. California Polytechnic State University, San Luis Obispo, 2020.

[3] F. Gasdia. Optical Tracking and Spectral Characterization of Cubesats for Operational Missions . Embry-Riddle Scholarly Commons, 2016.

[4] M. Yost and A. Zizzi. LEO SSA at the SpOT Facility. Astronautical Sciences Astrodynamics Conference, 167, 2019.

[5] S. Scuro D. Mortari and C. Bruccoleri. Attitude and Orbit Error in n- Dimensional Spaces. The Journal of the Astronautical Sciences, 54(304), 2006.

[6] A. Schaeperkoetter. A Comprehensive Comparison Between Angles-Only Initial Orbit Determination Techniques. Texas A&M University, 2011.